Published in final edited form as:
Carbohydr Polym. 2017 January 20; 156: 364–371. doi:10.1016/j.carbpol.2016.09.037.

Structure-activity relationship of the exopolysaccharide from a psychrophilic bacterium: a strategy for cryoprotection

Angela Casillo[a], **Ermenegilda Parrilli**[a], **Filomena Sannino**[a], **Daniel E. Mitchell**[b], **Matthew I. Gibson**[b], **Gennaro Marino**[a], **Rosa Lanzetta**[a], **Michelangelo Parrilli**[c], **Sandro Cosconati**[d], **Ettore Novellino**[e], **Antonio Randazzo**[e], **Maria L. Tutino**[a], and **M. Michela Corsaro**[a,*]

[a]Department of Chemical Sciences, University of Naples "Federico II", Complesso Universitario Monte S. Angelo, Via Cintia 4, 80126 Naples, Italy

[b]Department of Chemistry and Warwick Medical School, University of Warwick, Coventry, CV4 7AL, UK

[c]Department of Biology, University of Naples "Federico II", Complesso Universitario Monte S. Angelo, Via Cintia 4, 80126 Naples, Italy

[d]DiSTABiF, Second University of Naples, Via Vivaldi 43, 81100 Caserta, Italy

[e]Department of Pharmacy, University of Naples "Federico II", Via D. Montesano, 49, 80131 Naples, Italy

Abstract

Microrganisms from sea ice, glacial and subglacial environments are currently under investigation due to their relevant ecological functions in these habitats, and to their potential biotechnological applications. The cold-adapted *Colwellia psychrerythraea* 34H produces extracellular polysaccharides with cryoprotection activity. We here describe the purification and detailed molecular primary and secondary structure of the exopolysaccharide (EPS) secreted by *C. psychrerythraea* 34H cells grown at 4°C. The structure was determined by chemical analysis and NMR. The trisaccharide repeating unit of the EPS is constituted by a N-acetyl quinovosamine unit and two residues of galacturonic acid both decorated with alanine. In addition, the EPS was tested *in vitro* showing a significant inhibitory effect on ice recrystallization. In-depth NMR and computational analysis suggest a pseudohelicoidal structure which seems to prevent the local tetrahedral order of the water molecules in the first hydration shell, and could be responsible of the inhibition of ice recrystallization.

As cell cryopreservation is an essential tool in modern biotechnology and medicine, the observations reported in this paper could pave the way for a biotechnological application of *Colwellia* EPS.

Keywords

Exopolymer; *Colwellia psychrerythraea* 34H; alanine decoration; NMR spectroscopy; cold-adaptation

* corsaro@unina.it (Maria Michela Corsaro).

Europe PMC Funders Author Manuscripts

1 Introduction

The cryosphere, covering about one-fifth of the surface of the Earth, comprises several components: snow, river and lake ice; sea ice; ice sheets, ice shelves, glaciers and ice caps; and frozen ground which exist, both on land and beneath the oceans (Vaughan et al., 2013). All these habitats, combining the low temperature and the low liquid water activity, are challenging for all the forms of life (Casanueva, Tuffin, Cary, & Cowan, 2010).

The interface between solid and liquid water is an important environment for the survival of life at low temperatures. This includes melt water cryoconite holes and brines, where energy sources such as sunlight and reduced chemical compounds support life (Boetius, Anesio, Deming, & Mikucki, 2015). These extreme environments are inhabited by microorganisms of all three domains of life. In particular, those belonging to Bacteria and Archea can be classified as psychrophilic and psychrotolerant (Deming, 2009). Psychrophiles predominate in marine ecosystems, where the abyssal oceanic waters are permanently cold (< 5°C), whereas cold-adapted microorganisms isolated from terrestrial environments are mostly considered as psychrotolerant (De Mayeer, Anderson, Cary, & Cowan, 2014).

All these microorganisms have devoleped strategies to thrive and proliferate in such inhospital environments (De Mayeer et al., 2014; Deming, 2009; Feller & Gerday, 2003). Archaea (Cavicchioli, 2006), yeasts (Buzzini, Branda, Goretti, & Turchetti, 2012), diatoms (Aslam, Cresswell-Maynard, Thomas, & Underwood, 2012), fungi (Tsuji et al., 2013), and bacteria (Chattopadhyay, Reddy, & Shivaji, 2014; Deming, 2010) share very similar mechanisms of adaptation to low temperature that comprise the overexpression of cold-shock, the presence of unsaturated and branched fatty acids that maintain membrane fluidity (Chattopadhyay, 2006), the different phosphorylation of membrane proteins and lipopolysaccharides (Carillo et al., 2011; Carillo et al., 2013; Casillo et al., 2015; Corsaro et al., 2004; Corsaro et al., 2008; Ray, Kumar, & Shivaji, 1994a; Ray, Kumar, & Shivaji, 1994b), and the production of cold-active enzymes (Huston, Methè, & Deming, 2004), antifreeze proteins (AFPs) and antifreeze glycoproteins (AFGPs), and cryoprotectants (Deming, 2009). Among cryoprotectants, carbohydrate-based extracellular polymeric substances (EPSs) have a pivotal role in cold adaptation, as they form an organic network within the ice, modifying the structure of brine channels and contributing in the enrichment and retention of microrganisms in ice (Krembs, Eicken, Junge, & Deming, 2002; Krembs, Eicken, & Deming, 2011; Ewert & Deming, 2013). In the sea ice several diatoms species and many bacteria produce copious amount of EPS which accumulate as thick gels around the cells (Ewert & Deming, 2013). In particular, abundant EPS production from cold-adapted microorganisms can alter the microstructure and the desalination process of growing ice (Krembs et al., 2011).

Microbial EPS are complex and large polymers, composed of three or four types of monosaccharides, including pentoses, hexoses, aminosugars and uronic acids. These monosaccharides can be assembled in linear or ramified repeating units, and can be decorated by sulphate, phosphate, organic acids, and, as recently shown, by aminoacids

(Carillo et al., 2015; Mancuso Nichols, et al., 2005a; Mancuso Nichols, Guezennec, & Bowman, 2005b).

While there is a body of information in the literature about the properties of these polymers (Carrión, Delgado, & Mercadè, 2015; Li, Zhou, Zhang, Wang, & Zhu, 2008; Qin, Zhu, Chen, Wang, & Zhang, 2007; Sung & Joung, 2007), only few structures of EPS from Arctic and Antarctic marine bacteria have been fully elucidated (Corsaro et al., 2004; Carillo et al., 2015; Liu et al., 2013). In addition, due to their ability to thrive in extreme environments, cold-adapted bacteria can be considered un untapped reservoir of molecules with a broad range of unexplored application.

Colwellia psychrerythraea 34H is an obligately marine and psychrophilic γ-proteobacterium, isolated from subzero Arctic sediments and found also in sea ice from the Antarctic (Methè et al., 2005). This strain has been reported to produce cryoprotectant carbohydrate polymers, EPS (Marx, Carpenter, & Deming, 2009) and capsular polysaccharide (CPS); in particular, our previous work has described the structure of CPS decorated with threonines, that mimicks anti-freeze glycoproteins (Carillo et al., 2015). In this paper we report the structure of the EPS, which hitherto was not elucidated (Marx et al., 2009). Furthermore we describe the anti-freeze properties and the conformation of the polymer.

2 Materials and methods

2.1 Cell growth

C. psychrerythraea 34H (Methè et al., 2005) was grown aerobically at 4 °C in Marine Broth medium (DIFCO 2216). When the liquid culture reached late exponential phase (OD_{600} = 2), cells were harvested by centrifugation for 20 min at 5000 rpm and 4 °C.

2.2 EPS purification

C. psychrerythraea strain 34H was grown at 4°C in Marine Broth medium; the bacteria were removed by centrifugation (11.4 g, 30 min, 4°C), and the supernatant (2 L) was dialyzed against water (Spectra-Por, cut-off 10-12000 Da) obtaining 1.9 g.

An amount of 200 mg of growth broth was hydrolyzed with 5% aqueous CH_3COOH (20 mL, 100 °C, 3 h). The resulting suspension was then centrifuged (11.4 g, 4 °C, 30 min). The pellet was washed twice with water, and the supernatant layers were combined and lyophilized (170 mg). The supernatant portion (160 mg) was then fractionated on a Sephacryl S-400 HR column (GE Healthcare, 1.5 × 95 cm, flow 16.8 mL/h, fraction volume 2.5 mL), eluted with 0.05 M ammonium hydrogen carbonate obtaining two fractions. The first, eluted with the void volume, contained a mixture of saccharidic material (11 mg), while the second was constituted by medium components.

The saccharidic portion was further purified on a Q-Sepharose fast flow ion exchange chromatography (GE Healthcare, 1 × 35 cm, flow rate 23 mL/h, fraction volume 2 mL) eluted with 0.1 to 1 M NaCl, obtaining a pure fraction containing the EPS (0.8 mg, yield 0.04%).

Europe PMC Funders Author Manuscripts

2.3 DOC-PAGE analysis

PAGE was performed using the system of Laemmli (Laemmli, 1970) with sodium deoxycholate (DOC) as detergent, as already reported (Carillo et al., 2015). LPS, CPS and EPS bands were visualized by Alcian blue staining, as previously described (Al-Hakim & Linhardt, 1990; Tsai & Frasch, 1982)

2.4 Sugar and amino acid analysis

Monosaccharides were analyzed as acetylated methyl glycosides, as already reported (Carillo et al., 2015). The absolute configuration of the sugars was determined by gas chromatography analysis of their acetylated (*S*)-2-octyl glycosides, while the absolute configuration of the amino acid residue was inferred by analyzing its butyl ester derivative (Carillo et al., 2015; Leontein, Lindberg, & Lönngren, 1978). All the samples were analyzed on an Agilent Technologies 6850A gas chromatograph equipped with a 5973N mass-selective detector, as already reported (Carillo et al., 2015).

2.5 NMR Spectroscopy

^{1}H and ^{13}C NMR spectra were recorded using a Bruker Avance 600 MHz spectrometer equipped with a cryoprobe. All two-dimensional homo- and heteronuclear experiments (double quantum-filtered correlation spectroscopy, DQF-COSY; total correlation spectroscopy TOCSY; rotating-frame nuclear Overhauser enhancement spectroscopy, ROESY; nuclear Overhauser effect spectroscopy, NOESY; distortionless enhancement by polarization transfer–heteronuclear single quantum coherence, ^{1}H–^{13}C DEPTHSQC; heteronuclear multiple bond correlation, ^{1}H–^{13}C HMBC; and 2D F2-coupled HSQC) were performed using standard pulse sequences available in the Bruker software. The mixing time for TOCSY experiment was 100 ms. NOESY experiments were performed at mixing times of 50, 70, 100, 150, and 200 ms, in order to identify genuine NOEs effects. Chemical shifts were measured at 310 K in D_2O. TOCSY (mixing time 100 ms) and NOESY (mixing time 150 and 200 ms) experiments were also performed in H_2O/D_2O 9:1.

2.6 Structure Calculations

A simplified model of the polysaccharide having five repetitions of the trisaccharide A-B-C was constructed through the carbohydrate builder within the Glycam web server, (http://www.glycam.com.) while the Ala residue attached to the galacturonic acid was constructed by the Maestro package of the Schroedinger Suite 2014. Restrained simulated annealing (SA) calculations were performed on M1 using the AMBER 14.0 package (Case et al., 2014) with sugars described by the latest GLYCAM06 force field (GLYCAM_06j-1) (Kirschner, et al., 2008); parameters for Ala residue were retrieved from the ff14sb force field within the AMBER 14.0 package as well as missing bond parameters. Parameters for restrained SA, clustering and GIST calculations are reports in Supporting information.

2.7 Ice Recrystallization Inhibition assay

Ice recrystallization inhibition was measured using a modified splat assay (Congdon, Notman, & Gibson, 2013). A 10 μL sample of hydrogel dissolved in PBS buffer (pH 7.4) was dropped 1.40 m onto a chilled glass coverslip sat on a piece of polished aluminium

placed on dry ice. Upon hitting the chilled glass coverslip, a wafer with diameter of approximately 10 mm and thickness 10 μm was formed instantaneously. The glass coverslip was transferred onto the Linkam cryostage and held at −6 °C under N_2 for 30 minutes. Photographs were obtained using an Olympus CX 41 microscope with a UIS-2 20×/0.45/∞/0–2/FN22 lens and crossed polarizers (Olympus Ltd, Southend on sea, UK), equipped with a Canon DSLR 500D digital camera. Images were taken of the initial wafer (to ensure that a polycrystalline sample had been obtained) and after 30 minutes. Image processing was conducted using Image J (http://imagej.net/), which is freely available. In brief, ten of the largest ice crystals in the field of view were measured and the single largest length in any axis recorded. This was repeated for at least three wafers and the average (mean) value was calculated to find the largest grain dimension along any axis. The average of this value from three individual wafers was calculated to give the mean largest grain size (MLGS). This average value was then compared to that of a PBS buffer negative control providing a way of quantifying the amount of IRI activity.

3 Results and Discussion

3.1 Cell growth, EPS extraction, purification and characterization

A previous investigation had showed the existence of extracellular polysaccharides in *Colwellia psycherythraea* 34H growth medium, with cryoprotectant function and apparent ice-affinity (Marx et al., 2009). Moreover, we found that *C. psychrerythraea* 34H cells were surrounded by a capsule (CPS), the structure of which mimics anti-freeze glycoproteins (AFGPs) (Carillo et al., 2015). Then, as the CPS can be found both as cell-membrane associated and released in the culture medium, we checked if the released polymeric carbohydrates were constituted exclusively by CPS.

C. psychrerythraea strain 34H was grown aerobically at 4°C in Marine Broth medium until late exponential phase, then the cells were separated from spent medium by gentle centrifugation. Both resulting fractions (i.e. cell pellet and culture supernatant) were kept and stored at -20°C. Both lipopolysaccharide (LPS), which is the major component of the outer leaflet of bacterial external membrane (Carillo et al., 2013), and CPS molecules (Carillo et al., 2015) were extracted and characterized. The culture supernatant was extensively dialyzed against distilled water, and the dialysate was lyophilized. Results of 14% DOC-PAGE experiments are shown in Fig. 1. Bands at low molecular masses, visualized by Alcian blue staining, attributable to LPS molecules were clearly detectable (Fig. 1, lane a), together with CPS bands at higher molecular masses (Fig. 1, lanes a and c). In addition, the Alcian blue visualized another group of bands not visible in the cells extraction (Fig. 1, lane a).

The GC-MS analysis of the monosaccharides derivatized as acetylated methyl glycosides (MGA), revealed that all the components of LPS and the CPS were present (Carillo et al., 2013; Carillo et al., 2015). In addition, the analysis showed the presence of 2-amino-2,6-dideoxyglucose (quinovosamine, QuiN) that was never identified before in the cells extracts of *Colwellia psychrerythraea*.

In order to purify the EPS, the dialysate cells supernatant was treated with acetic acid to dissociate micellar aggregates of LPS, CPS and EPS. This procedure allows for the separation of the saccharidic piece of LPS from the lipid A, the glycolipid moiety of the LPS, the phosphate groups of which could be responsible of saline bridges through divalent cations with the anionic polysaccharides. Hence, after hydrolysis and centrifugation, the supernatant mixture was preliminarily purified on size exclusion chromatography. Two main peaks were obtained: the first, eluted in the void volume, contained the higher molecular weight compounds, corresponding to CPS and EPS, while the second one contained the core oligosaccharide of LPS, and growth medium components not excluded from the dialysis tubes (data not shown). The polysaccharides mixture, constituted by CPS and EPS, was then chromatographed on an Q-Sepharose fast flow (GE Healthcare) ion exchange chromatography column, eluting with a NaCl gradient from 0.1 up to 1M. A pure fraction of EPS, eluted with 500 mM NaCl, was obtained (Fig. 1, lane b). The gel also indicated for the EPS a molecular weight higher than CPS (Carillo et al., 2015), due to the higher migration distance of EPS respect to the dye front of the gel (Fig. 1, lanes b and c). This time, the GC-MS analysis of MGA showed the presence of GalA and QuiN as the main components, together with a signal assignable to an alanine residue, on the basis of the comparison with a pure standard. A D-configuration was determined for both monosaccharides, whereas the alanine residue showed a L-configuration. EPS polysaccharide was then analyzed by homo- and heteronuclear 2D NMR spectroscopy. In particular, ^{1}H-^{1}H DQF-COSY (double quantum-filtered correlation spectroscopy),^{1}H-^{1}H TOCSY (total correlation spectroscopy), ^{1}H-^{1}H NOESY (nuclear Overhauser enhancement spectroscopy), ^{1}H-^{13}C DEPT-HSQC (distortionless enhancement by polarization transfer-heteronuclear single quantum coherence), ^{1}H-^{13}C HMBC (heteronuclear multiple bond correlation) and 2D F*2*-coupled HSQC experiments were performed. The DEPT-HSQC spectrum (Fig. S1 and Table) displayed the presence of three anomeric cross-peaks at δ 5.54/100.9 (**A**), 4.98/100.8 (**B**), and 4.56/103.5 ppm (**C**). The anomeric configuration of the residues was established by the one bond ^{13}C-^{1}H couplings constants ($^{1}J_{C1\text{-}H1}$) measured in a 2D F*2*-coupled HSQC experiment (Fig. S2), that suggested an α-configuration for residues **A** and **B** (185 Hz and 177 Hz, respectively), and a β-configuration for residue **C** (164 Hz). These configurations were further supported by a NOESY experiment (Fig. S3). Residues **A** and **B** were recognized as *galacto*-configured residues based on the presence of cross-peaks from H-1 up to H-4 in the TOCSY spectrum (Fig. S4).

Then, in the NOESY spectrum, starting from H-4, the H-5 resonance was identified. Both these residues were assigned to 4-substituted galactopyranuronic acids since their C-4 signals were shifted downfield (δ 77.9 ppm for **A** and δ 79.4 ppm for **B**, respectively) with respect to that of an unsubstituted galacturonic acid (Bock & Pedersen, 1983). In both residues, H-5 proton signals showed in the HMBC experiment (Fig. S5a) a long-range scalar connectivity with the C-6 carboxyl signals at δ 170.2 ppm and δ 171.0 ppm, for residues **A** and **B** respectively. These last values were up-field shifted with respect to the reference value (Bock & Pedersen, 1983), thus indicating that these carboxyl groups were involved in amide linkages. Indeed, two additional spin systems of alanine residues were present. In particular, resonances at δ 4.23/52.0 and δ 1.39/19.2 ppm for the spin system Ala (**D**) and 4.22/52.2 and 1.42/19.2 ppm for the spin system Ala (**E**), attributable to CH and CH_3 groups,

respectively, were found (Fig. S1). Finally, carboxyl groups at δ 180.3 ppm and 181.2 ppm, for **D** and **E** respectively, were revealed by the long range scalar couplings in the HMBC experiment (Fig. S5a and b). Residue **B** was linked to C-4 position of residue **A,** as deduced from the HMBC experiment which displayed a long range scalar correlation between H-1 of **B** at δ 4.98 ppm and C-4 of **A** at δ 77.9 ppm (Fig. S5a). The correlations present in COSY and TOCSY (Fig. S4) spectra indicated a *gluco*-configuration for residue **C**, that was then identified as a β-N-acetyl-quinovosamine, since in the ^{1}H-^{13}C DEPT-HSQC experiment its H-2 correlated with a nitrogen bearing carbon at δ 56.0 ppm (Fig. S1). In particular, NOESY experiment measured in H_2O/D_2O (Fig. 2) revealed a NOE contact between the N-H at δ 8.39 ppm and H-2 of **C**, that in turn correlated with the methyl group at δ 1.91 ppm.

Finally, this last signal showed a long range scalar connectivity with the carbonyl signal at δ 175.9 ppm in the HMBC experiment (Fig. S5b). Furthermore, C-3 resonance of the same residue, was shifted downfield (δ 81.2 ppm, Fig. S1 and Table) with respect to that of an unsubstituted quinovosamine residue (Corsaro et al., 2006; Knirel et al., 1987), suggesting a glycosidic linkage at this position.

In fact, this carbon signal displayed a long range scalar connectivity in the HMBC spectrum with H-1 of residue **A** (δ 5.54 ppm), indicating that this last was linked to the C-3 position of **C**. Residue **C,** in turn, was linked to C-4 position of **B**, in agreement with a long range scalar connectivity between H-1 of **C** at δ 4.56 ppm and C-4 of **B** at δ 79.4 ppm. The monosaccharides sequence was confirmed by dipolar couplings revealed in the NOESY spectrum (Fig. S3).

Finally, the substitution of the two carboxyl groups of **A** and **B** by alanine aminoacids **D** and **E**, respectively, was deduced by NOESY (Fig. 2) and TOCSY (Fig. S6) data measured in H_2O/D_2O. In particular, the amide linkage between C-6 of residue **B** and alanine **E** was revealed from a NOE contact between the amino acid N-H (δ 7.70 ppm), identified in the TOCSY experiment, and both H-5 and H-4 signals of residue **B** (δ 4.90 and 4.30 ppm, respectively). In the same way, the NOE contact between N-H of **D** (δ 7.91 ppm) and H-5 of **A** (δ 4.28 ppm) confirmed the substitution of **A**. All the above data indicated for EPS from *Colwellia psychrerythraea* 34H a trisaccharidic repeating unit, as illustrated in Fig. 3.

3.2 Three-Dimensional Structure Characterization

With the aim of assessing the three-dimensional arrangement of EPS, structural information were retrieved by NMR data and employed in molecular dynamics simulations. The NOE connectivities in the NOESY spectra between 1,3-diaxial protons (H-3 and H-5 of **A** and **B**, and H-1/H-3/H-5 and H-2/H-4 of **C**, Fig. S3), unambiguously indicated that all three sugar moieties assume the classical $^{4}C_1$ chair conformation. Therefore, dihedral angle constraints were used to keep the sugar in this conformation during structure calculations. NOESY spectra also showed interesting inter-residue NOEs that are diagnostic for the determination of the general conformation of the polysaccharide. Particularly, strong NOEs between H-1 of **A**, **B** and **C** and H-4 of **C**, **A** and **B**, respectively, along with strong NOEs between H-1 of **A** and H-3/H-5 of **C**, weak NOEs between H-1 of **B** and H-3/H-5 of **A**, and between H-1 of **C** and H-3/H-5 of **B** indicate the relative spatial orientation of the sugars (Fig. S3). The lack of

long-range NOEs indicates that the overall structure of the polysaccharide is fairly linear. These structural information were employed to construct a model of the EPS polysaccharide through restrained molecular dynamics simulations. However, the molecular weight of the purified EPS is higher than CPS molecules (Carillo et al., 2015), therefore, following the strategy already applied in a previous study on CPS (Carillo et al., 2015), also in this case we decided to construct and simulate a simplified model of the EPS structure. Most precisely, a simplified model made up by five repetition of the trimer **A**-**B**-**C** was constructed resulting in a 15-mer structure. An ensemble of 200 isoenergetic structures was calculated featuring for all the considered distances a maximum violation of 0.4 Å. Subsequently, these different conformations were clustered considering the sugar ring atoms of the three central repeats with root-mean-squared difference (rmsd) value of 1.5 Å. The choice to disregard the terminal repeats from the clustering was dictated by the fact that these are less representative of the whole conformational behavior of the polysaccharide. By clustering the 200 conformations of our model system, 14 different clusters were obtained in which cluster number 1 represented the 83% of the total ensemble demonstrating a good convergence of our calculations toward a well-defined structure. For this cluster, the representative conformation was considered (i.e. the one closest to the centroid of the cluster) for further 310 K MD simulations aimed at probing the thermodynamic stability in explicit solvent and assessing the behavior of water molecules around the considered structure. From this analysis, it was clear that the three central repeats adopt a fairly linear conformation that roughly resembles a left-handed helix (Fig. 4a).

This conformation seems to be stabilized by a series of inter residue H-bond interactions. Of particular interest is the formation of a H-bond between the amide nitrogen of the N-acetyl quinovosamine (residue **C**) and the carbonyl oxygen of the adjacent galacturonic acid (residue **B**). Indeed the β-glycosidic linkage of residue **C** forces the aforementioned atoms in closed vicinity so as to make this interaction possible (Fig. 4b). Additional polar interactions are further established by the alanine attached to residue **B** and the C2 hydroxy group of residue **A**. These interactions seem to play a prominent role in the induction of a pseudo helicoidal structure and would lock the conformation of the amino acid with respect to the sugar skeleton. Thus, these studies would outline the importance of three structural features: i) the amide nitrogen of quinovosamine, ii) the specific β-glycosidic linkage of this residue, and ii) the presence of the alanine attached to the galacturonic acid.

While the aforementioned MD simulations were critical to probe the stability of the modeled structure in explicit solvent they were also crucial in the study of the interaction of the polysaccharide with the water itself. In particular, MD data were analyzed to estimate the thermodynamic values for the water molecules interacting with our polysaccharide through the Grid Inhomogeneous Solvation Theory Method (GIST) developed by Nguyen et al. (2012).This method enables for the characterization of each region around the solute with respect to its water occupancy, the energetic interaction with other water molecules and the solute, and its entropic contribution. Herein, these data allowed us to visualize the regions of the modeled polysaccharide that are more positively contacted by water molecules. In particular, by calculating the density weighted solute-water interaction energy (kcal/mol/A^3) it was possible to visualize the regions where water molecules are found to have more

favorable interactions with the polysaccharide (Fig. 5a). These calculations suggest that the specific conformation induced by the polar interactions described would allow for the energetically favored presence of a water molecule in the cage formed by residue **C** and its adjacent residues **A** and **B** (before and after, respectively); as expected additional favorable solute-water interactions areas are placed around the alanine carboxylate groups (Fig. 5a).

Moreover, in this conformation **C** exposes its hydrophobic face to the solvent resulting in unfavorable interactions. The trapping of water molecules in the aforementioned cage is further outlined by visualizing the density weighted translational and orientational entropy maps (Fig. 5b and c). Based on these observations, the effect of the polysaccharide on the structural order of waters in the vicinity was also evaluated. To this end, the tetrahedral order parameter Q_k was also calculated (Errington & Debenedetti, 2001); this is a measure of the propensity of a particular water molecule and its four neighboring molecules to adopt a tetrahedral arrangement. In this case, negative Q_k values were detected in the sugar cage described above indicating no tetrahedral geometry of water molecules in this area (Fig. 5d). Alteration of water ability to adopt such an arrangement could be at the basis for the antifreeze properties of EPS. Interestingly, similar results were also achieved for some antifreeze glycoproteins by Mallajosyula et al. (2014) who demonstrated that these perturbation effects are propagated to distant hydration layers.

3.3 Ice Recrystallization Inhibition

To assess any cryoprotective effect of this polysaccharide, ice recrystallization inhibition (IRI) activity was measured. Antifreeze proteins, antifreeze glycoproteins and severval synthetic polymers have been shown to be potent IRI's (Congdon et al., 2013; Gibson, 2010). IRI has been linked to survival in frozen environments and applied to cellular cryopreservation (Deller, Vatish, Mitchell, & Gibson, 2014; Mitchell, Cameron, & Gibson, 2015). To test this, a modified 'splat' assay was used. Briefly, 10 μL droplets of the polysaccharide in PBS was dropped down a tube into a cooled (~ -70 °C) glass cover slip, and then transferred to a microscope set at – 6 °C. After 30 minutes, the mean largest grain size (MLGS) was measured and reported relative to a PBS control. It is worth considering that in this assay, MLGS values below ~ 20 % indicate zero growth (as the initial crystals cannot have zero size). The activity of the EPS is reported in Fig. 6. A positive control (polyvinyl alcohol, PVA) and negative control (polyethylene glycol, PEG) were also used. In the concentration range reported, there was a clear inhibition of ice growth, which is rather unique to this polysaccharide. For example, dextran cyclodextrins and other saccharides have little or no IRI (Deller, Vatish, Mitchell, & Gibson, 2013).

4 Conclusions

In this study, the full characterization of the EPS primary structure and molecular dynamics simulations have revealed a unique strategy for cold adaptation of *Colwellia psychrerythraea* 34H. The repeating unit is constituted by a N-acetyl-quinovosamine unit and two residues of galacturonic acid both decorated with alanine amino acids. In-depth NMR and computational analysis suggest a pseudohelicoidal structure which seems to prevent the local tetrahedral order of the water molecules in the first hydration shell. Quantitative ice

recrystallization inhibition (IRI) assays were employed to link the structural characterization of the polysaccharide, its influence on local water structure and ice growth interactions. Interestingly, the EPS IRI activity is comparable to the activity of synthetic polymer mimics of antifreeze proteins, which have been found to confer cryoprotective effects (Mitchell et al., 2015) suggesting that EPS plays a role in cold-survival. More intriguingly, the suggested helical structure is similar to that observed in antifreeze glycoproteins (AFGP) – it should be noted that there is no crystal structure of AFGP but a polyproline-type helix is observed in circular dichroism spectroscopy and NMR (Tachibana et al., 2004). A second feature of AFP and AFGP is the presence of distinct hydrophobic and hydrophilic regions which are crucial for IRI activity. The hydrophobic face of the N-acetyl quinovosamine could contribute to this activity alongside potential water ordering, as seen in AFPs (Sun, Lin, Campbell, Allingham, & Davies, 2014). In consideration that very few macromolecules have been reported to have IRI activity, the observations reported in this paper are rather significant, thus showing all the potential use of this polymer as a cryoprotectant.

Supplementary Material

Refer to Web version on PubMed Central for supplementary material.

Acknowledgements

This work was supported by a Research Project Grant from the Royal Society. DEM acknowledges the EPSRC for a studentship from the MOAC Doctoral Training Centre; grant number EP/F500378/1. MIG thanks the ERC for a Starting Grant, CRYOMAT 638661. The authors thank the BioTekNet for the use of 600 MHz NMR spectrometer.

References

Al-Hakim A, Linhardt RJ. Isolation and recovery of acidic oligosaccharides from polyacrylamide gels by semi-dry electrotransfer. Electrophoresis. 1990; 11:23–28. [PubMed: 1690641]

Aslam SN, Cresswell-Maynard T, Thomas DN, Underwood GJC. Production and characterization of the intra- and extracellular carbohydrates and polymeric substances (EPS) of the three sea-ice diatom species, and evidence for a cryoprotective role for EPS. Journal of Phycology. 2012; 48:1494–1509. [PubMed: 27009999]

Bock K, Pedersen C. Carbon- 13 nuclear resonance spectroscopy of monosaccharides. Advances in Carbohydrate Chemistry and Biochemistry. 1983; 41:27–66.

Boetius A, Anesio AM, Deming JW, Mikucki JA. Microbial ecology of the cryosphere: sea ice and glacial habitats. Nature Reviews Microbiology. 2015; 13:677–690. [PubMed: 26344407]

Buzzini P, Branda E, Goretti M, Turchetti B. Psychrophilic yeasts from worldwide glacial habitats: diversity, adaptation strategies and biotechnological potential. FEMS Microbiology Ecology. 2012; 82:217–241. [PubMed: 22385361]

Carillo S, et al. Structural investigation and biological activity of the lipooligosaccharide from the psychrophilic bacterium *Pseudoalteromonas haloplanktis* TAB 23. Chemistry-A European Journal. 2011; 17:7053–7060.

Carillo S, et al. Structural characterization of the core oligosaccharide isolated from the lipopolysaccharide of the psychrophilic bacterium *Colwellia psychrerythraea* strain 34H. European Journal of Organic Chemistry. 2013; 18:3771–3779.

Carillo S, et al. A unique capsular polysaccharide structure from the psychrophilic marine bacterium *Colwellia psychrerythraea* 34H that mimics antifreeze (Glyco)proteins. Journal of the American Chemical Society. 2015; 137:179–189. [PubMed: 25525681]

Carrión O, Delgado l, Mercadè E. New emulsifying and cryoprotective exopolysaccharide from Antarctic *Pseudomonas* sp. ID1. Carbohydrate Polymers. 2015; 117:1028–1034. [PubMed: 25498731]

Casanueva A, Tuffin M, Cary C, Cowan DA. Molecular adaptations to psychrophily: the impact of 'omic' technologies. Trends in Microbiology. 2010; 18:374–381. [PubMed: 20646925]

Case, DA., et al. AMBER. 14th ed. University of California; San Francisco: 2014.

Casillo A, et al. Structural investigation of the oligosaccharide portion isolated from the lipooligosaccharide of the permafrost psychrophile *Psychrobacter arcticus* 273-4. Marine Drugs. 2015; 13:4539–4555. [PubMed: 26204948]

Cavicchioli R. Cold-adapted archaea. Nature Reviews Microbiology. 2006; 4:331–343. [PubMed: 16715049]

Chattopadhyay MK. Mechanism of bacterial adaptation to low temperature. Journal of Biosciences. 2006; 31:157–165. [PubMed: 16595884]

Chattopadhyay MK, Reddy GS, Shivaji S. Psychrophilic bacteria: biodiversity, molecular basis of cold adaptation and biotechnological implications. Current Opinion in Biotechnology. 2014; 3:100–116.

Congdon TC, Notman R, Gibson MI. Antifreeze (Glyco)protein mimetic behavior of poly(vinyl alcohol): detailed structure ice recrystallization inhibition activity study. Biomacromolecules. 2013; 14(5):1578–1586. [PubMed: 23534826]

Corsaro MM, et al. Influence of growth temperature on lipid and phosphate contents of surface polysaccharides from the Antarctic bacterium *Pseudoalteromonas haloplanktis* TAC 125. Journal of Bacteriology. 2004; 186:29–34. [PubMed: 14679221]

Corsaro MM, et al. Structural determination of the O-Chain polysaccharide from the lipopolysaccharide of the haloalkaliphilic *Halomonas pantelleriensis* bacterium. European Journal of Organic Chemistry. 2006; 7:1801–1808.

Corsaro MM, et al. Highly phosphorylated core oligosaccaride structures from cold-adapted *Psychromonas arctica*. Chemistry-A European Journal. 2008; 14:9368–9376.

De Mayeer P, Anderson D, Cary C, Cowan DA. Some like it cold: understanding the survival strategies of psychrophiles. EMBO Reports. 2014; 15:508–517. [PubMed: 24671034]

Deller RC, Vatish M, Mitchell DA, Gibson MI. Ice recrystallisation inhibition by polyols: comparison of molecular and macromolecular inhibitors and role of hydrophobic units. Biomaterial Science. 2013; 1:478–485.

Deller RC, Vatish M, Mitchell DA, Gibson MI. Synthetic polymers enable non-vitreous cellular cryopreservation by reducing ice crystal growth during thawing. Nature Communications. 2014; 5(3244):1–6.

Deming, JW. Extremophiles: cold environments. Encyclopedia of Microbiology. Schaechter, M., editor. Elsevier; 2009. p. 147-158.

Deming, JW. Sea ice bacteria and viruses. Sea Ice. 2th ed. Thomas, DN.; Dieckmann, GS., editors. Oxford: Blackwell Science Ltd; 2010. p. 247-282.

Errington JR, Debenedetti PG. Relationship between structural order and the anomalies of liquid water. Nature. 2001; 409:318–321. [PubMed: 11201735]

Ewert M, Deming JW. Sea Ice microorganisms: environmental constraints and extracellular response. Biology. 2013; 2:603–628. [PubMed: 24832800]

Feller G, Gerday C. Psychrophilic enzymes: hot topics in cold adaptation. Nature Reviews Microbiology. 2003; 1:200–208. [PubMed: 15035024]

Gibson MI. Slowing the growth of ice with synthetic macromolecules: beyond antifreeze (glyco)proteins. Polymer Chemistry. 2010; 1:1141–1152.

Huston AL, Methè BA, Deming JW. Purification, characterization, and sequencing of an extracellular cold-active aminopeptidase produced by marine psychrophile *Colwellia psychrerythraea* strain 34H. Applied and Environmental Microbiology. 2004; 70:3321–3328. [PubMed: 15184127]

Kirschner KN, et al. GLYCAM06: A generalizable biomolecular force field. Carbohydrates. Journal of Computational Chemistry. 2008; 29:622–655. [PubMed: 17849372]

Knirel YA, et al. Somatic antigens of *Pseudomonas aeruginosa* The structure of the O-specific polysaccharide chain of the lipopolysaccharide from *P. aeruginosa* O13. European Journal of Biochemistry. 1987; 163:627–637. [PubMed: 3104040]

Krembs C, Eicken H, Deming JW. Exopolymer alteration of physical properties of sea ice and implications for ice habitability and biogeochemistry in a warmer Arctic. Proceedings of the National Academy of Sciences USA. 2011; 108:3653–3658.

Krembs C, Eicken H, Junge K, Deming JW. High concentrations of exopolymeric substances in Arctic winter sea ice: implications for the polar ocean carbon cycle and cryoprotection of diatoms. Deep Sea Research Part I: Oceanographic Research Papers. 2002; 49:2163–2181.

Laemmli UK. Cleavage of structural proteins during the assembly of the head of bacteriophage T4. Nature. 1970; 227:680–685. [PubMed: 5432063]

Leontein K, Lindberg B, Lönngren J. Assignment of absolute configuration of sugars by g.l.c. of their acetylated glycosides from chiral alcohols. Carbohydrate Research. 1978; 62:359–362.

Li WW, Zhou WZ, Zhang YZ, Wang J, Zhu XB. Flocculation behavior and mechanism of an exopolysaccharide from the deep-sea psychrophilic bacterium *Pseudoalteromonas* sp. SM9913. Bioresource Technology. 2008; 99:6893–6899. [PubMed: 18353634]

Liu SB, et al. Structure and ecological roles of a novel exopolysaccharide from the Arctic sea ice bacterium *Pseudoalteromonas* sp. Strain SM20310. Applied and Environmental Microbiology. 2013; 79(1):224–230. [PubMed: 23087043]

Mallajosyula SS, et al. Perturbation of long-range water dynamics as the mechanism for the antifreeze activity of antifreeze glycoprotein. The Journal of Physical Chemistry B. 2014; 118(40):11696–706. [PubMed: 25137353]

Mancuso Nichols CA, et al. Chemical characterization of exopolysaccharides from Antarctic marine bacteria. Microbial Ecology. 2005; 49:578–589. [PubMed: 16052372]

Mancuso Nichols CA, Guezennec J, Bowman JP. Bacterial exopolysaccharides from extreme marine environments with special consideration of the Southern ocean, sea ice, and deep-sea hydrothermal vents: a review. Marine Biotechnology. 2005b; 7:253–271. [PubMed: 16075348]

Marx JD, Carpenter SD, Deming JW. Production of cryoprotectant extracellular polysaccharide substances (EPS) by the marine psychrophilic bacterium *Colwellia psychrerythraea* strain 34H under extreme conditions. Canadian Journal of Microbiology. 2009; 55:63–72. [PubMed: 19190702]

Methè BA, et al. The psychrophilic lifestyle as revealed by the genome sequence of *Colwellia psychrerythraea* 34H through genomic and proteomic analyses. Proceedings of the National Academy of Sciences USA. 2005; 102:10913–10918.

Mitchell DA, Cameron NR, Gibson MI. Rational, yet simple, design and synthesis of an antifreeze-protein inspired polymer for cellular cryopreservation. Chemical Communication. 2015; 51:12977–12980.

Nguyen CN, et al. Grid inhomogeneous solvation theory: Hydration structure and thermodynamics of the miniature receptor cucurbituril. The Journal of Chemical Physics. 2012; 137:044101. [PubMed: 22852591]

Qin G, Zhu L, Chen X, Wang PG, Zhang Y. Structural characterization and ecological roles of a novel exopolysaccharide from the deep-sea psychrotolerant bacterium *Pseudoalteromonas* sp. SM9913. Microbiology. 2007; 153:1566–1572. [PubMed: 17464071]

Ray MK, Kumar GS, Shivaji S. Phosphorylation of membrane proteins in response to temperature in an Antarctic *Pseudomonas syringae*. Microbiology. 1994a; 140:3217–3223. [PubMed: 7881543]

Ray MK, Kumar GS, Shivaji S. Phosphorylation of lipopolysaccharides in the Antarctic psychrotroph *Pseudomonas syringae*: a possible role in temperature adaptation. Journal of Bacteriology. 1994b; 176:4243–4249. [PubMed: 8021210]

Sun T, Lin FH, Campbell RL, Allingham JS, Davies PL. An antifreeze protein folds with an interior network of more than 400 semi-clathrate waters. Science. 2014; 343(6172):795–798. [PubMed: 24531972]

Sung JK, Joung HY. Cryoprotective Properties of Exopolysaccharide (P-21653) Produced by the Antarctic Bacterium, *Pseudoalteromonas arctica* KOPRI 21653. The Journal of Microbiology. 2007; 45:510–514. [PubMed: 18176533]

Tachibana Y, et al. Antifreeze glycoproteins: elucidation of the structural motifs that are essential for antifreeze activity. Angewandte Chemie International Edition in English. 2004; 43(7):856–62.

Tsai CM, Frasch CE. A sensitive silver stain for detecting lipopolysaccharides in polyacrylamide gels. Analytical Biochemistry. 1982; 119:115–119. [PubMed: 6176137]

Tsuji M, et al. Cold adaptation of fungi obtained from soil and lake sedimentin the Skarvsnes ice-free area, Antarctica. FEMS Microbiology Letters. 2013; 346:121–130. [PubMed: 23862768]

Vaughan, DG., et al. Observations: Cryosphere. Climate Change 2013: The Physical Science Basis. Contribution of Working Group I to the Fifth Assessment Report of the Intergovernmental Panel on Climate Change. Stocker, TF., et al., editors. Cambridge University Press; Cambridge: 2013. p. 317-382.

Europe PMC Funders Author Manuscripts

Europe PMC Funders Author Manuscripts

Highlights

- Cryoprotectans are used to preserve the cellular damages due to freeze-thaw cycles.
- Biotechnological production of new cryoprotectans is demanding.
- *Colwellia psychrerythraea* 34H produces a cryoprotectant exopolysaccharide.
- The exopolisaccharide (EPS) primary and secondary structure has been finely characterised.
- The molecular dynamics simulations (MD) suggest how the pseudohelicoidal structure inhibits the first hydration shell.

Europe PMC Funders Author Manuscripts

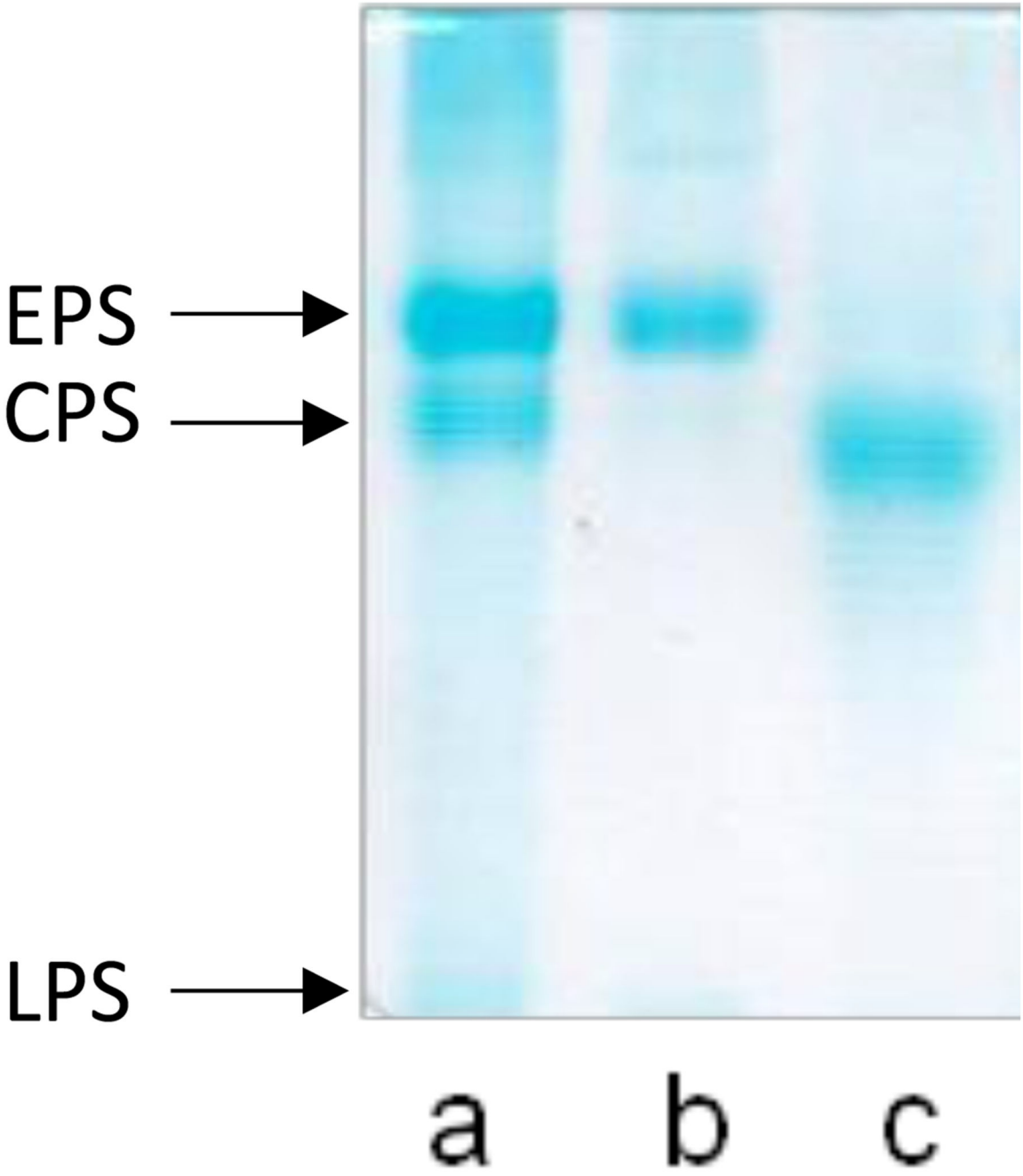

Fig. 1.
Analysis of the EPS fraction from *Colwellia psychrerythraea* 34H by 14% DOC-PAGE. The gel was stained with Alcian blue. (a) dialysate broth, (b) purified EPS from growth broth, and (c) purified CPS from cells.

Europe PMC Funders Author Manuscripts

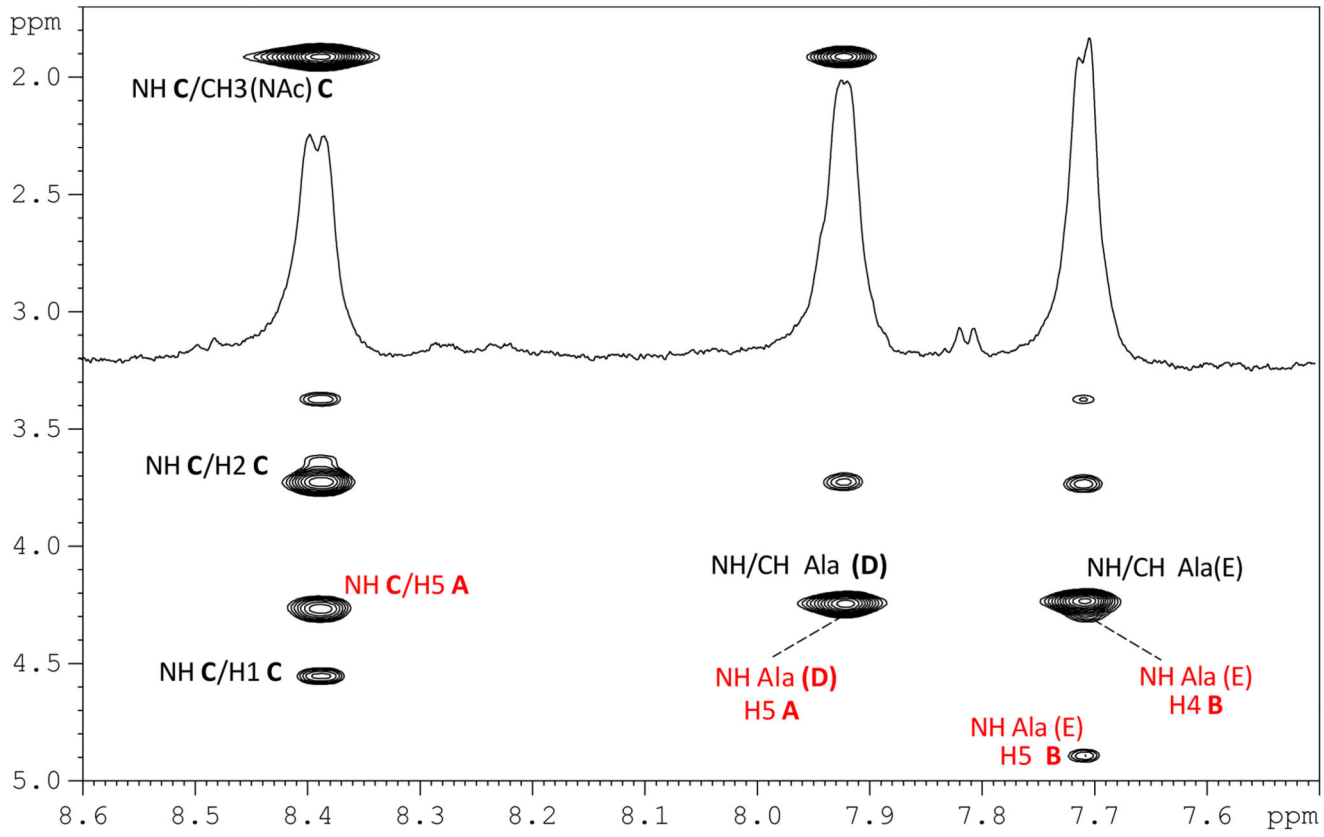

Fig. 2.

Expansion of the ^{1}H-^{1}H NOESY spectrum together with the corresponding ^{1}H spectrum of EPS from *C. psychrerythraea* 34H. The spectrum was performed in H_2O/D_2O 9:1 at 310K. NH relevant cross-peaks for alanines **D** and **E**, and quinovosamine **C**. Correlations' attribution follows the letters system of Table; in black and red are reported intra-residues and inter-residues correlations, respectively.

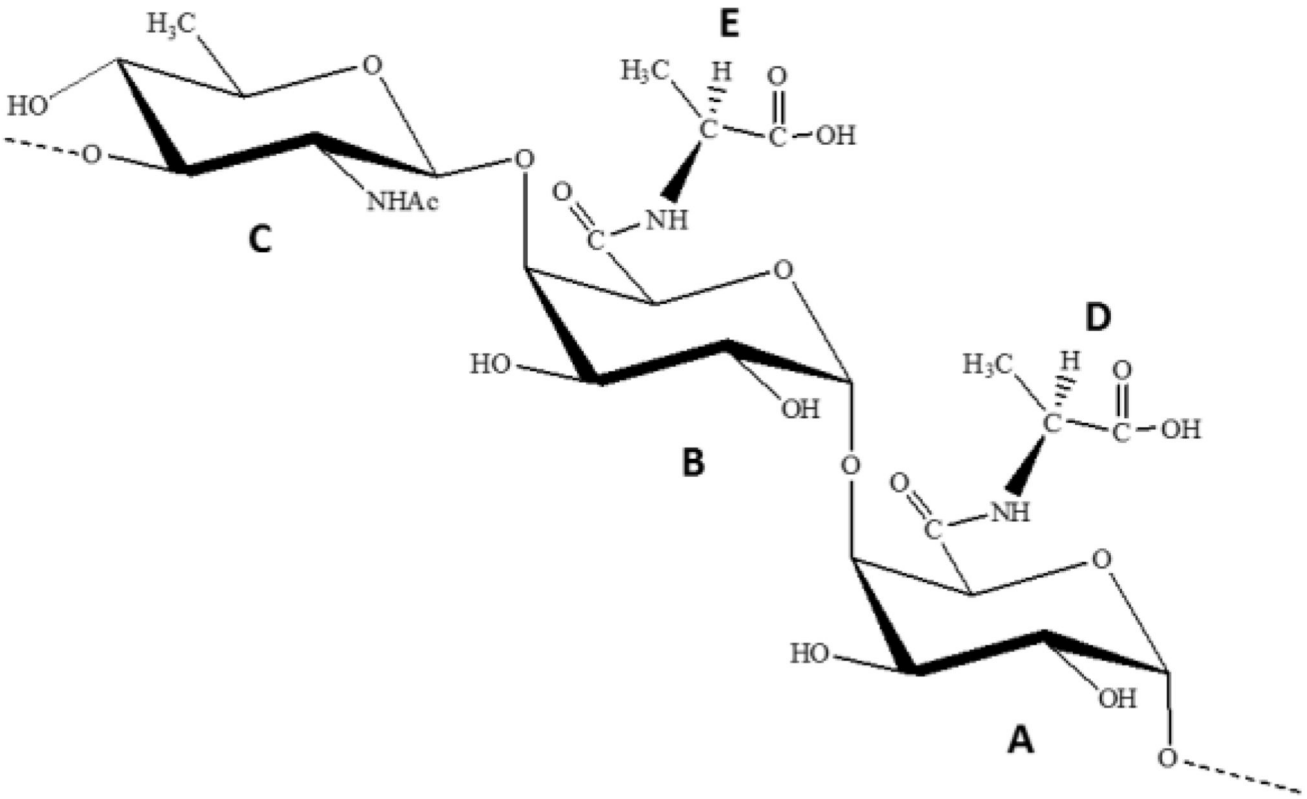

Fig. 3.
Primary repeating trisaccharide structure of the EPS produced by *C. psychrerythraea* 34H.

Europe PMC Funders Author Manuscripts

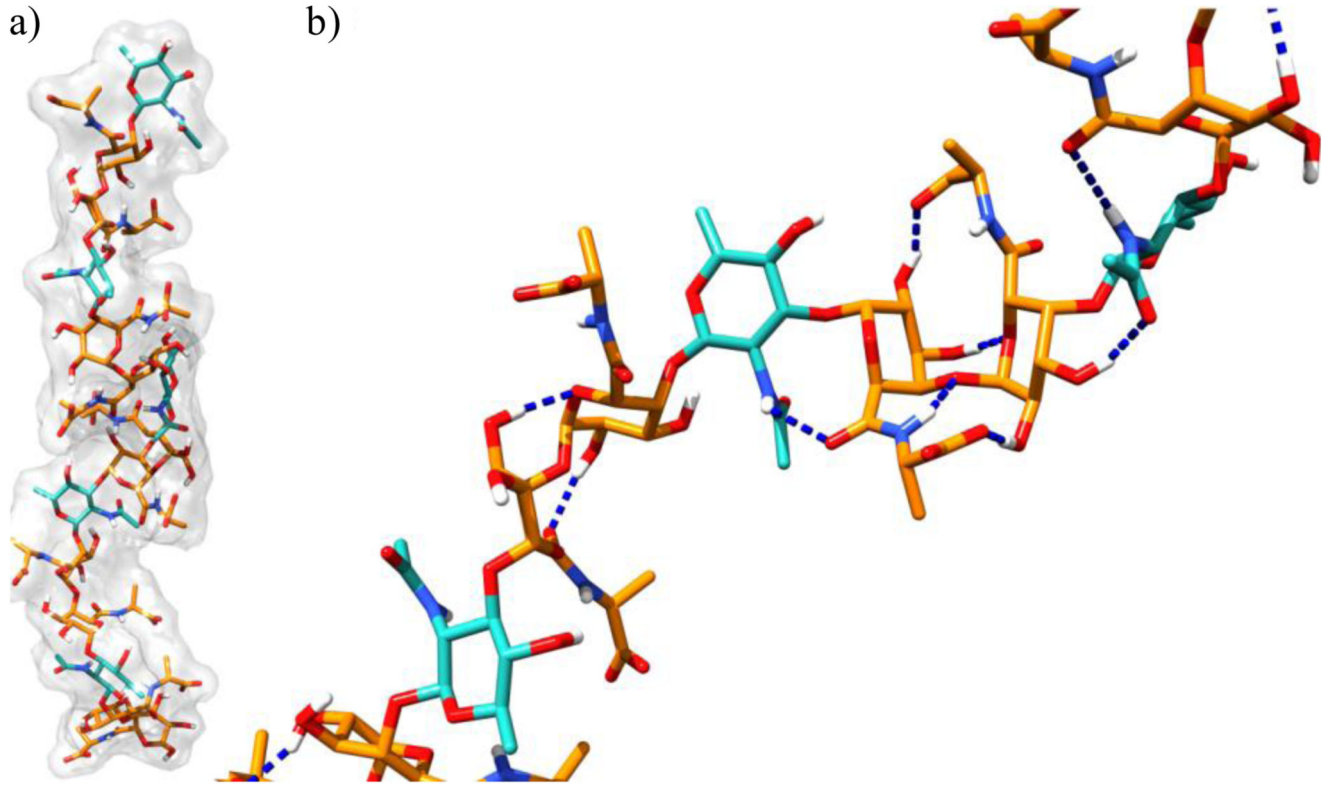

Fig. 4.

Front (a) and zoomed (b) view of the representative structure of EPS as calculated by restrained SA calculations. Residues **A** and **B** are represented as orange sticks while residue **C** as cyan sticks. H-bonds are represented as dashed blue lines.

Europe PMC Funders Author Manuscripts

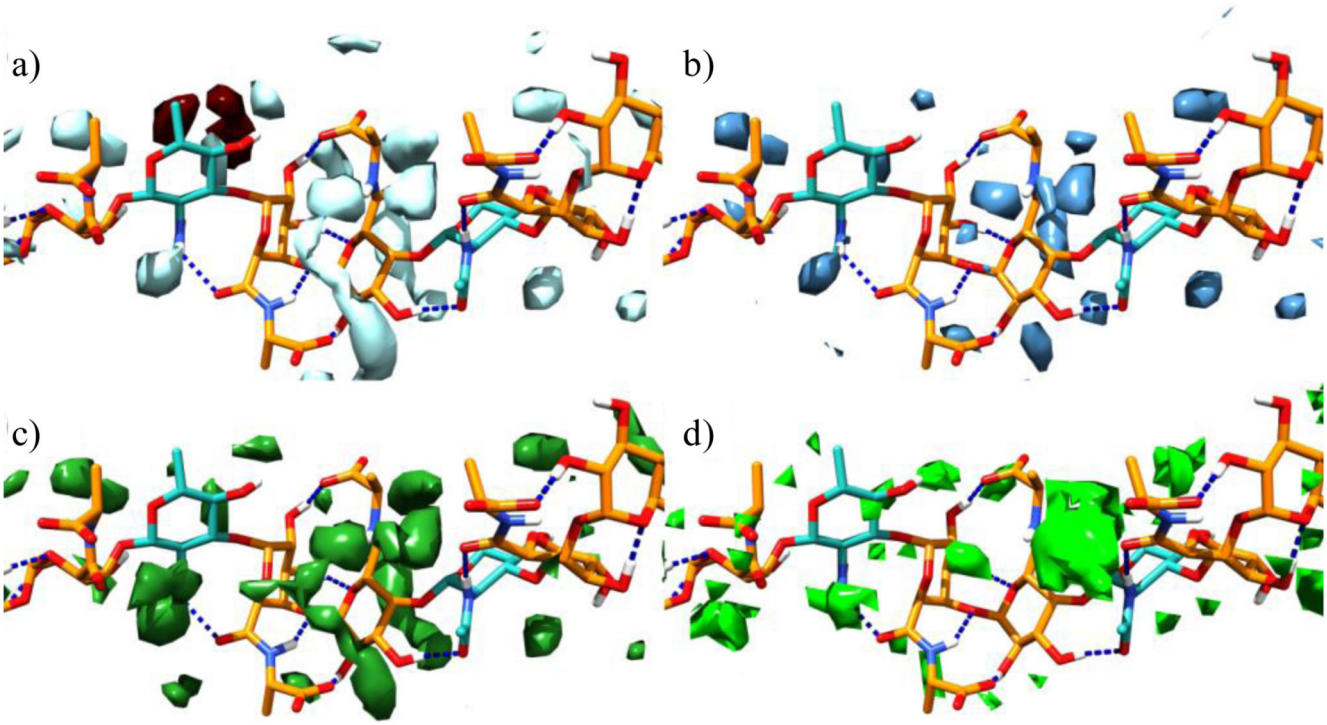

Fig. 5.

Average structure of EPS polysaccharide deriving from the 20 ns MD production run (a-d). Residues **A** and **B** are represented as orange sticks while residue **C** as cyan sticks. Cyan and brown surfaces in (a) represent the regions of the density weighted solute-water interaction energy for an isovalue of 0.67 kcal/mol/A^3. Panels (b) and (c) report the density weighted translational (blue surfaces) and orientational entropy (dark green surfaces) maps at an isovalue -0.06 kcal/mol/A^3, respectively. Panel (d) reports the regions around the solute were a Tetrahedral Order Parameter (Q_k) for surrounding waters has a value of -0.02, meaning no tetrahedral arrangement of water molecules.

Europe PMC Funders Author Manuscripts

Europe PMC Funders Author Manuscripts

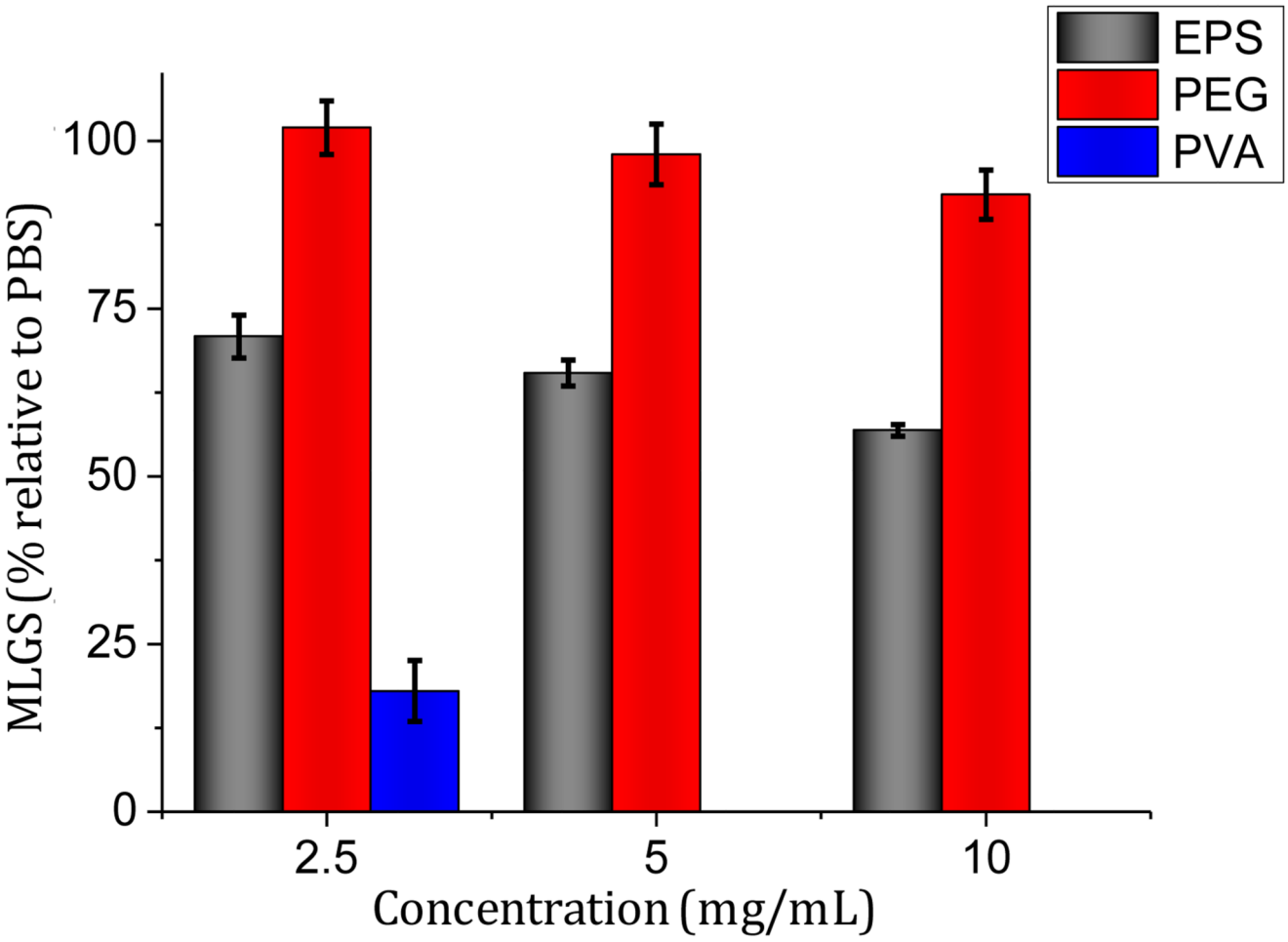

Fig. 6.

Ice Recrystallization Inhibition activity of EPS from *C. psychrerythraea* 34H was compared with PEG, used as a negative control, and PVA as a positive. Mean largest grain size is expressed as a percentage of PBS buffer, and small MLGS value indicate increased IRI activity.

Europe PMC Funders Author Manuscripts

Table

^{1}H and ^{13}C NMR assignments of EPS from *C. psychrerythraea* 34H. Spectra were recorded in D_2O at 310K at 600 MHz using acetone as external standard (δ_H/δ_C 2.22/31.5 ppm).

Residue	H1	H2	H3	H4	H5	H6
	C1	C2	C3	C4	C5	C6
A	5.54	3.87	3.97	4.46	4.28	-
4-α-D-Gal*p*A6LAla(**D**)	100.9	69.0	69.8	77.9	72.0	170.2
B	4.98	3.63	3.95	4.30	4.90	-
4-α-D-Gal*p*A6LAla(**E**)	100.8	69.6	70.7	79.4	73.0	171.0
C	4.56	3.74	3.72	3.39	3.37	1.27
3-β-D-Qui*p*NAc	103.5	56.0	81.2	77.7	72.5	18.4

Additional chemical shifts:
NAc: at δ 1.91/24.0 (CH_3), 175.9 (CO)
Ala (D): at δ 4.23/52.0 (CH), 1.39/19.2 (CH_3), 180.3 (COOH), 7.91 (NH, H_2O/D_2O)
Ala (E): at δ 4.22/52.2 (CH), 1.42/19.2 (CH_3), 181.2 (COOH), 7.70 (NH, H_2O/D_2O)